Indian Journal of Pure & Applied Physics
Vol. 56, November 2018, pp. 853-858

Characterization and photoluminescence of Dy^{3+} doped $CaTiO_3$ nanoparticles prepared by sol-gel method

Punam Thakur[a], S J Khambadkar[a], Avish Patil[a], C M Dudhe[a,b]*, Pooja Thombare[a] & A A Chaudhary[a]

[a]Department of Physics, Institute of Science, R T Road, Nagpur 440 001, India

[b]Department of Physics, Government Science College, Gadchiroli 442 605, India

Received 24 May 2017; accepted 15 May 2018

A modified sol-gel route using tetra isopropyl ortho titanate and calcium acetate under the catalytic action of nitric acid has been presented for the synthesis of Dy^{3+} doped $CaTiO_3$ nanoparticles. Various instrumentation techniques like, thermo gravimetric analysis, X-ray diffraction, Fourier transform infrared spectroscopy, ultraviolet-visible spectroscopy, transmission electron microscopy and photoluminescence spectroscopy have been employed to characterize the compound. It has been found that described method is much better than earlier reported methods, as it improves the morphology, particle size and homogeneity of $CaTiO_3$ nanoparticles. By this method we obtain sphere-like particles of average size ~42 nm which falls among the least known sizes of pure and doped $CaTiO_3$ nanoparticles. The spectroscopic parameters like band-gap energy and intense $^4F_{9/2} \rightarrow {}^6H_{13/2}$ transition on account of Dy^{3+} doping show excellent agreements with the reported data in the literature.

Keywords: Perovskite, Sol-gel synthesis, UV-Vis spectroscopy, Photoluminescence, Transmission electron microscopy

1 Introduction

$CaTiO_3$ is a naturally occurring first mineral-perovskite and hence is the flag-bearer of the perovskite family. Its room temperature phase is primitive orthorhombic and belongs to the space group *Pcmn*(62)[1]. This space group is centro symmetric in nature with Ti atom at the centre of oxygen octahedron. However, the octahedron is not perfectly regular because of variable orientations of neighboring octahedra in the structure[1]. The centro symmetric nature makes $CaTiO_3$ different many ways from the other non centro symmetric and widely investigated family members like $BaTiO_3$, $KNbO_3$, $PbTiO_3$, and so on[1,2]. Conceivably, lack of non centro symmetry made the compound less striking as compared to other perovskites at early stage of the research as far as researchers' interest is concerned. However, later stages various applications of $CaTiO_3$ in semiconductors, photocatalysis and memory devices have been explored[3-6]; moreover, it acts as a potential candidate for negative temperature coefficient (NTC) - type thermistor[7,8] due to its conducting nature above[1] 300 °C. These interesting applications develop an adequate interest in $CaTiO_3$, now-a-days.

Recent studies documented that $CaTiO_3$ is an excellent host material for rare earth impurities as far as photoluminescence applications are concerned[9-11]. It is found that doping of these impurities in a small quantity does not disturb the structural properties especially of $CaTiO_3$ compound on account of its structural stability over the wide range of temperature. Hence to enhance other applications and to make compound prolific, doping in this compound is preferable. Furthermore, nanoscale effect may bring some interesting changes in properties as compared to the bulk counterparts. Thus, considering all these aspects, instead of pure compound, a Dy^{3+}-doped $CaTiO_3$ compound in nanoparticles form was synthesized by a sol-gel route, and various characterizations and photoluminescence (PL) application were studied.

Compounds of $CaTiO_3$ can be synthesized by many ways. The usual high-temperature sintering technique affects the size of the particles and mostly micron or submicron size of particles are obtained[4,8]. Low temperature methods on the other hand seem to be more suitable in this regard. Various low temperature synthesis techniques like sol–gel[10-12] combustion[13], polymeric precursor[14,15], organic–inorganic solution[16], co-precipitation and hydrothermal[17] were used for the synthesis of $CaTiO_3$ based compounds, but size,

*Corresponding author (E-mail: chandraguptadudhe@gmail.com)

morphology and homogeneity of the particles prepared by many of these methods is not up to the mark of satisfaction. In many of these methods mostly calcium nitrate was used as a direct source of Ca ion; however, in the present method, we used calcium acetate in reaction with nitric acid. Interestingly, in contrast to the recent report regarding the use of acetic acid as a chelating agent in $CaTiO_3$ leads to micrometric particles and heterogeneous composition[18], we successfully synthesized homogeneous nano sized particles. Because of this achievement, the method is presented here along with some characterizations. We feel that the $CaTiO_3$ nanoparticles synthesized by our method might be a suitable candidate for size-based applications, such as photocatalysis and nanodevices in electronic industry.

2 Experimental

Synthesis of nanoparticles of $Ca_{0.95}TiO_3:Dy_{0.05}$ was carried out by a sol-gel process using AR grade tetra isopropyl ortho titanate ($C_{12}H_{28}O_4Ti$; Sigma-Aldrich), calcium acetate hydrated ($C_4H_6CaO_4xH_2O$; LOBA Chemie), dysprosium oxide (Dy_2O_3; IRE, India), acetic acid glacial (CH_3COOH; Merck), concentrated HNO_3 (Merck), ethyl alcohol (C_2H_5OH; Scientific Australia) and polyvinyl alcohol ($[-C_2H_4O]_n$; LOBA Chemie) compounds. They were used without any further purification.

The sol-gel process was carried out at room temperature. At first, 23.94 mL of $C_{12}H_{28}O_4Ti$ was hydrolyzed in 84 mL mixture solution of ethyl alcohol and acetic acid taken in the ratio of 3:1. Another mixture solution was prepared by dissolving 12.86 g of $C_4H_6CaO_4$ x H_2O in 80 mL distilled water and 0.746 g of Dy_2O_3 in12 mL concentrated HNO_3, and mixing together by using magnetic stirrer for 2 h. This mixture solution was added into the first solution and further stirred for 1 h. This process gives a clear and transparent solution. In this solution, polyvinyl alcohol (PVA) (3 g/dl) solution (prepared by dissolving 0.192 g of PVA in 64 mL distilled water) was added drop-wise in the volume ratio of 5:2 and stirred further for 1 h. This final solution was kept at rest for 12 h to form a milky-white gel.

The gel was then incubated in an oven maintained at 70 °C, for 2-3 days. The dried precursor called as xerogel was obtained by this procedure.

The xerogel was first characterized by thermo gravimetric (TG) analysis. The 'Shimatzu' spectrometer (TG/DTA, Shimatzu, DTG-60) was used for the study. This study defines the phase formation temperature. Using obtained TG/DTA characteristic and keeping in mind our recent experience[19,20] about good crystalline nature and X-ray diffraction peaks pattern of nanoparticles prepared at slightly higher calcined temperature, the xerogel was calcined at reasonably higher temperature, i.e. at 750 °C, for 4 h.

X-ray diffraction (XRD) data of synthesized compound was recorded by using X-ray diffractometer (D8 Advance, Bruker, Germany) employing CuK_α radiation (1.5406 Å) in the 2θ range of 15-85°. Fourier transform -infrared (FTIR) spectra of the compound was recorded by using a spectrometer FTIR-8400S (Shimadzu). Nanocrystalline nature of the compound was confirmed by transmission electron microscopy (TEM) (TEM CM200, Philips). UV-Vis spectrum of the compound was recorded by using spectrometer (UV-Vis 1700, Shimatzu, Japan). The pellets of the compound required for such measurements were prepared by mixing the powder with a few drops of 1 wt% solution of polyvinyl alcohol as a binder and then pressing isostatically under the pressure of 5-6 t for 5 min. Before to use, they were heat-treated at 700 °C for 5 h to remove the binder, and polished mechanically. The photoluminescence excitation and emission spectra of the synthesized nanoparticles were recorded by using a spectroflurometer (F-7000, Hitachi, Japan).

3 Results and Discussion

Figure 1 shows the TG/DTA spectra of the precursor of as synthesized Dy^{3+} doped $CaTiO_3$ compound. The DTA curve showed three endothermic and three

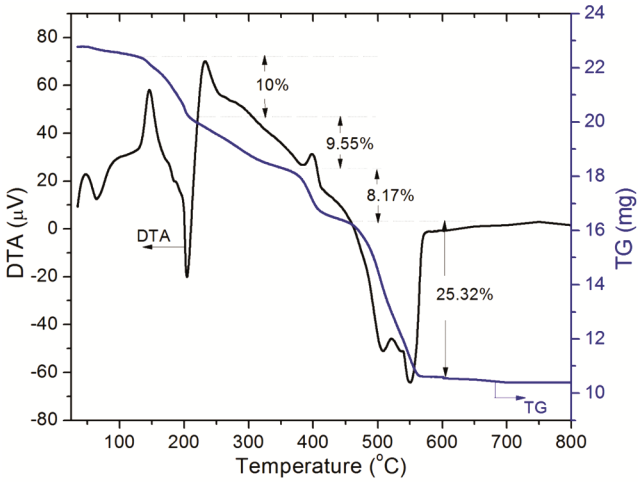

Fig. 1 — Thermogravimetric (TG/DTA) curves for Dy^{3+} doped $CaTiO_3$ precursor.

exothermic peaks, indicating that various organic compounds were decomposed and gases evolved out from the precursor at different stages during the calcination. Correspondingly, TG curve showed four stages of weight loss. These observations suggest that molecular changes happening during the decomposition are quite complicated. The total weight loss was found to be ~53%. The pattern of TG/DTA curve is found very much similar to the Pr, Al doped $CaTiO_3$ precursor as reported by Yin *et al.*[9], however corresponding peaks and weight losses were occurred at relatively lower temperatures. This lowering in temperatures might be responsible for improving the size of the particles. Above 570 °C, stationary curves were obtained which is a sign of completion of reaction and formation of orthorhombic phase of the compound.

As described in above section, to obtain better XRD peaks pattern and crystallinity, the calcination was carried out at 750 °C. The X-ray diffraction spectrum of the prepared Dy^{3+} doped $CaTiO_3$ compound at this calcined temperature is shown in Fig. 2. This peaks pattern matches with the JCPDS File No. 22-0153; indicating that the compound stabilizes in orthorhombic phase. The lattice parameters as determined by least squares fit method

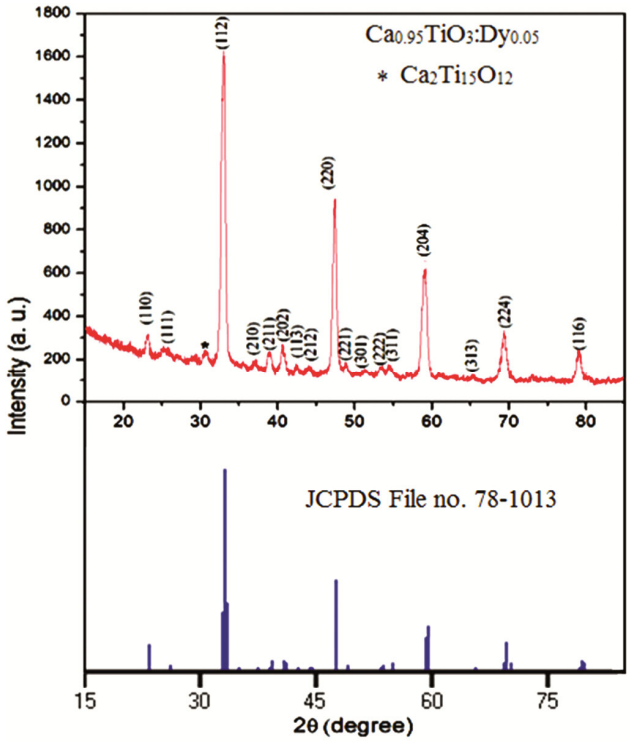

Fig. 2 — X-ray diffraction pattern of as prepared Dy^{3+} doped $CaTiO_3$ compound along with JCPDS pattern.

using structural formula: $\frac{1}{d^2_{hkl}} = \frac{h^2}{a^2} + \frac{k^2}{b^2} + \frac{l^2}{c^2}$ (where *h, k* and *l* are miller indices, *a, b* and *c* are lattice parameters and d_{hkl} is the interplaner spacing) were found as *a* =5.443 Å, *b*= 5.399 Å and *c*=7.695 Å. These values are in good agreement with the values reported for orthorhombic bulk $CaTiO_3$ (JCPDS File No.22-0153).

The literature survey also suggest that Dy^{3+} ions replace Ca^{2+} ions[11,21,22]. By far in the present study, equivalent Ca^{2+} ionic vacant sites were structurally made available for such impurity ions. The XRD pattern also showed no peaks corresponding to Dy_2O_3. These observations suggest that, impurity ions are occupying the Ca^{2+} vacant sites properly in orthorhombic cell.

Structural characteristics were also done by FTIR spectroscopy. Figure 3 shows the FTIR and spectrum of the $CaTiO_3$ compound. In Fig. 3 only two significant vibration bands are observed; one at around 1490 cm^{-1} and the other at 544 cm^{-1}. The vibration centered at 1490 cm^{-1} can be assigned to the stretching vibration of C=O which may be due the adsorption of trace of CO on the surface of particles during the synthesis. A strong band centered at 544 cm^{-1} can be assigned to the stretching and/or bending vibration of O-Ti-O. This spectrum coincides with the spectrum reported by Li *et al.*[23] for Nd^{3+} doped $CaTiO_3$ nanofibers.

Figure 4(a) is the transmission electron microscopy (TEM) image of the synthesized Dy^{3+} doped $CaTiO_3$ compound. This figure reveals nanocrystalline nature of the particles. The particles are irregular spheres and agglomerated. The particle size distribution

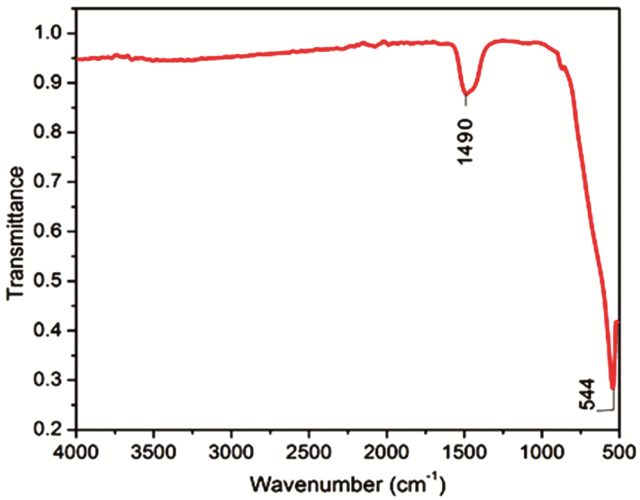

Fig. 3 — FTIR spectrum of the synthesized compound.

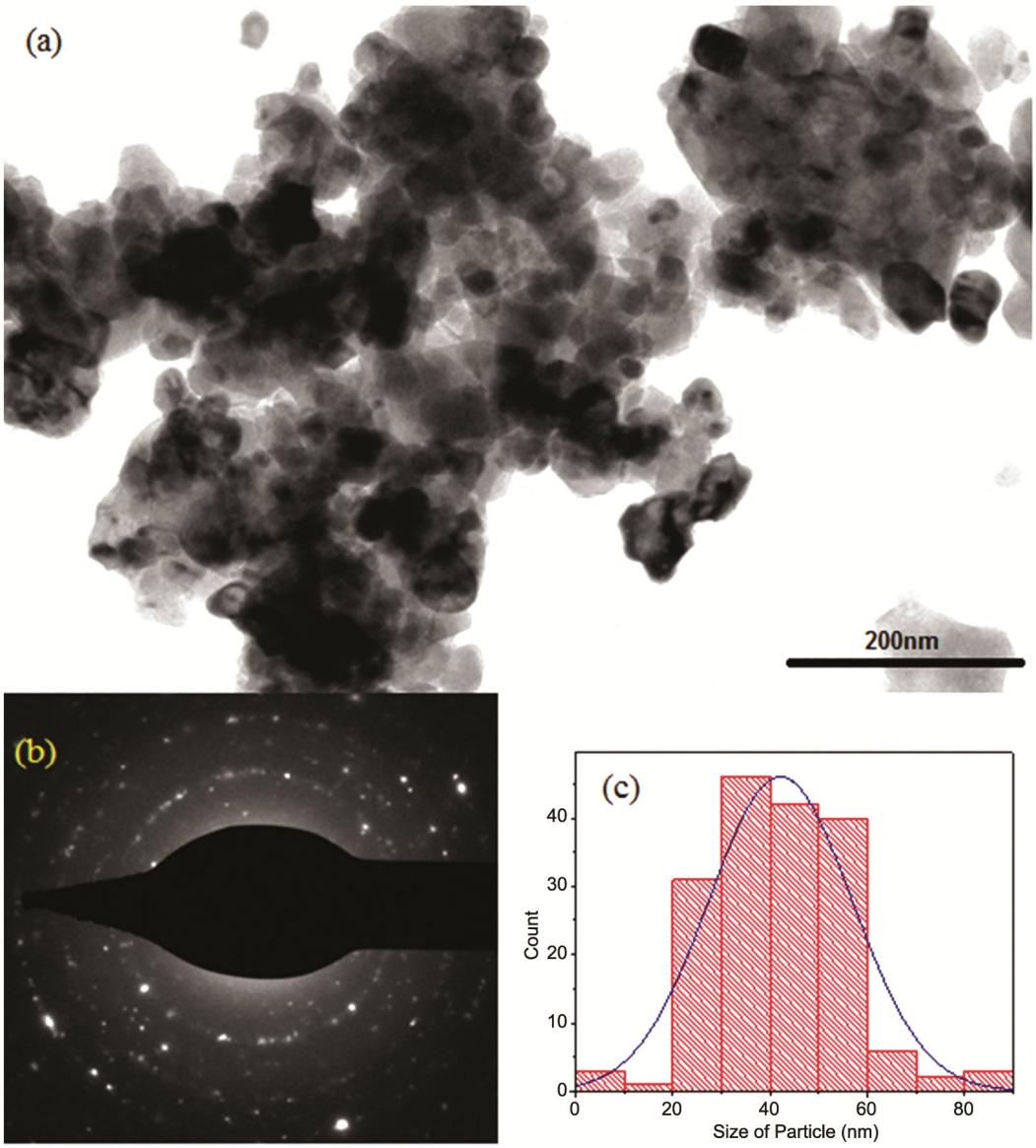

Fig. 4 — (a) TEM and (b) selected area electron diffraction pattern of the compounds confirming nanocrystalline nature, and (c) particle distribution curve.

curve is shown in Fig. 4(c) which clearly give the average size of the particle is about 42 nm. To the best of our knowledge, this is one of the smallest reported sizes for $CaTiO_3$ nanopaticles. The size of the particles is also calculated from the XRD pattern by Debye Scherer formula: $D = k\lambda/\beta\cos\theta$, where D is the average particle size, k = constant (~0.9), β is the full width at half the maximum of the peak in radian and λ is the wavelength of X-rays. The size of the particles is calculated for five major peaks (112), (220), (204), (224) and (116) corresponding to which the sizes of the particles, respectively, comes out to be 13, 15.5, 12.3, 15.3 and 16.6 nm. The average size of the particles is 14.5 nm, which is smaller than that estimated by TEM. The discrepancy can be assigned to the agglomeration of the particles.

Figure 4(b) is the selected area electron diffraction (SAED) pattern of the compound. The pattern is spotty rings. This is a sign of crystalline nature. The well-defined XRD peaks as seen in Fig. 2(a) also support the finding of crystalline nature.

Ultraviolet-visible (UV-Vis) spectrum of the synthesized doped compound is shown in Fig. 5(a). The absorption edge is about 347 nm. The estimation of direct and indirect optical band gap energy is done by using Kubelka-Munk (K-M) transform spectra

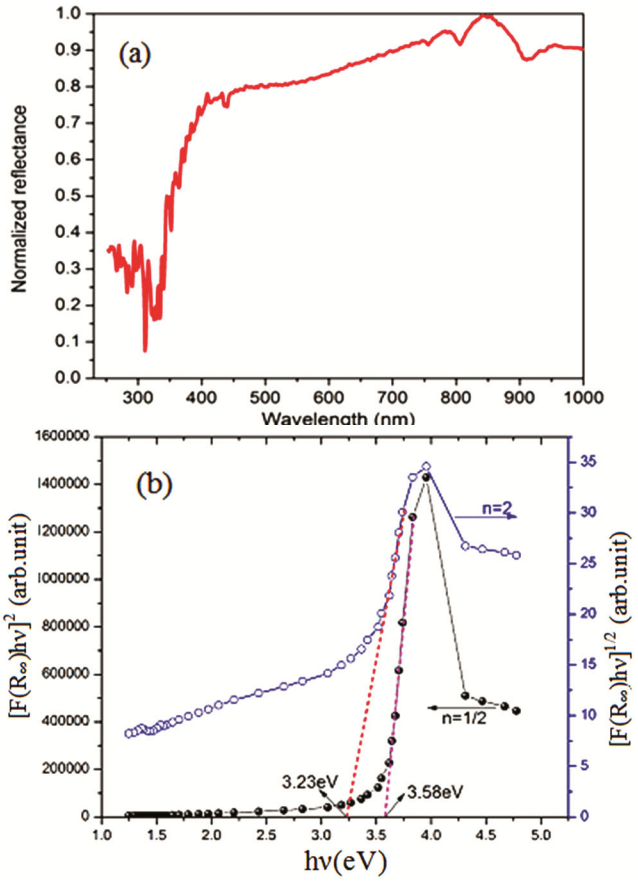

Fig. 5 — (a) UV-Vis spectrum and (b) Kubelka-Munktrans for spectrum of the synthesized Dy^{3+} doped $CaTiO_3$ nanoparticles.

(Fig. 5(b)). It is the graph between $1/n^{th}$ power of the product of K-M function and photon energy ($h\nu$) against $h\nu$. The details of formulation are discussed in our previous papers[19,20]. It is found that the direct band gap (n=1/2) energy, i.e., difference between the upper energy level of conduction band (CB) and the upper energy level of valence band (VB) is about 3.58 eV, which is matching with the reported values[24]. The indirect band gap (n=2) energy, i.e., the difference between the lower energy level of CB and upper energy level of VB was found to be ~3.23 eV. Thus the bandwidth of CB is about 0.35 eV. These values of band gap energies can make the present nanoparticles suitable for photon (light) related activities like photocatalysis and photoluminescence.

Lemanski and Deren[11] found that the strongest PL emission occurs in Dy^{3+} doped $CaTiO_3$ for 1 mol% concentration. According to them, the cross-relaxation processes might be activated for higher concentration and the PL will be quenched. To verify this result, the PL characterization of the present 5 at% Dy^{3+} doped

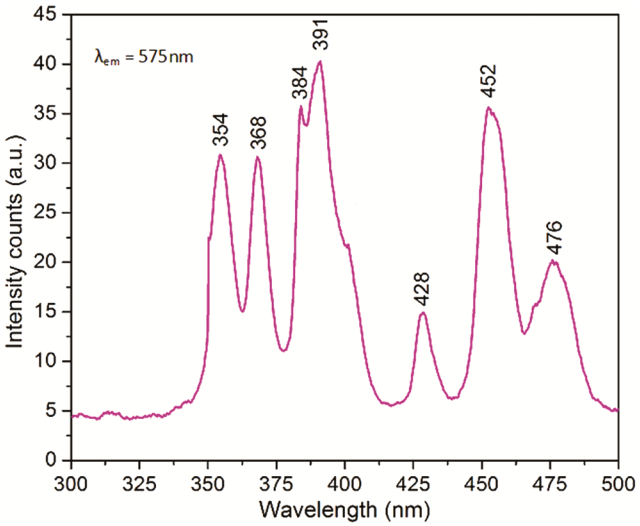

Fig. 6 — Excitation spectra of as prepared Dy^{3+} doped $CaTiO_3$ nanoparticles.

$CaTiO_3$ was studied. The study is limited to the most intense emission band originates from the $^4F_{9/2} \rightarrow {}^6H_{13/2}$ transition, because of instrumental limitations.

The excitation spectra of the compound for λ_{em} =575 nm in the range of 300-500 nm is shown in Fig. 6. This spectrum is similar to the Dy^{3+}-doped $Y_4Al_2O_9$ and Dy^{3+}-doped alumino fluoro borophosphate compounds reported by Boruc *et al.*[25] and Vijaykumar *et al.*[26], respectively; indicating that the spectrum as seen in Fig. 6 is the representative characteristics excitation of Dy^{3+}. However, relative intensities and peaks positions in the present compound are slightly different than the above reported spectra. It is found that the positions of excitation peaks in the present case are greatly matched with the Dy^{3+} doped $LiNbO_3$ compound[27]. This concludes that the host lattice has a certain effect on the excitation characteristics of Dy^{3+}. The similarity with the $LiNbO_3$ may be due to presence of BO_6 (B= Ti, Nb) octahedral. Such octahedra are not reported in $Y_4Al_2O_9$ or alumino fluoro borophosphate compounds[25,26]. By comparison with Dy^{3+} doped $LiNbO_3$ compound[27], the spectral terms and absorption wavelength of the present study are related as: $^4I_{11/2} + {}^4P_{7/2} \rightarrow$ 354 nm, $^4M_{19/2} + {}^4P_{5/2} \rightarrow$ 368 nm, $^4F_{7/2} + {}^4I_{13/2} + {}^4M_{21/2} \rightarrow$ 391 nm, $^4G_{11/2} \rightarrow$ 428 nm, $^4F_{15/2} \rightarrow$ 452 nm and $^4F_{9/2} \rightarrow$ 476 nm.

As $^4F_{9/2} \rightarrow {}^6H_{13/2}$ transition is the intense one, the emission spectrum is recorded for excitation wavelength of $^4F_{9/2}$. Figure 7 shows the emission spectrum of the present sample. It comprises a single emission peak at around 575 nm, which is similar to the reported by Vijaykumar *et al.*[26] in alumino fluoro

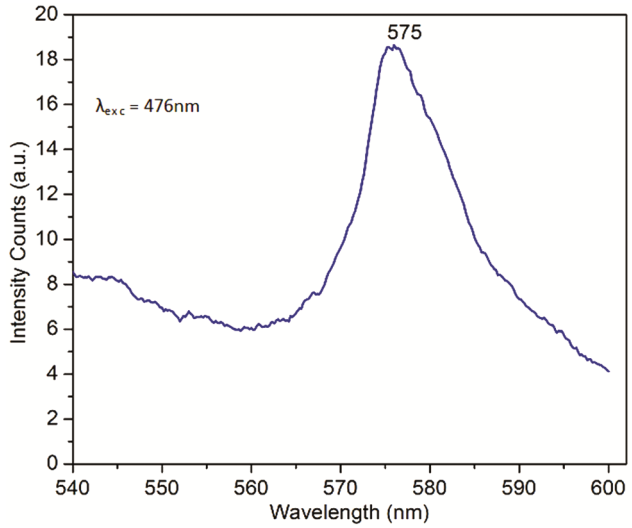

Fig. 7 — Emission spectra of Dy^{3+} doped $CaTiO_3$ nanoparticles.

boro phosphate. It was found that the significant minor emission peaks as observed by Lemanski and Deren[11] within the wavelength region 555-600 nm in 1%, 3.5% and 0.5% Dy^{3+} doped $CaTiO_3$compounds are disappearing in the present case. This may be due to strengthening of quenching, indicating the influence of higher concentration of Dy^{3+} on PL properties.

4 Conclusions

A sol-gel route using tetra isopropyl ortho titanate and calcium acetate under the catalytic action of nitric acid is successfully employed for the synthesis of Dy^{3+} doped $CaTiO_3$ nanoparticles. These nanoparticles are characterized by excellent particle size, morphology and homogeneity. The spectroscopic parameters like band-gap energy, intense $^4F_{9/2} \rightarrow {}^6H_{13/2}$ transition on account of Dy^{3+} doping, etc. show excellent agreement with the reported data in the literature. Because of the improved size and being lead-free they may be further used for the enhancement in particle size based phenomenon like photocatalysis, and for nanodevices in electronic industry.

References

1 Megaw H D, *Ferroelectricity in crystals*, (Methuen Press: London), 1957.

2 Sakhya A P, Maibam J, Saha S, Chanda S, Dutta A, Sharma B I, Thapa R K & Sinha T P, *Indian J Pure ApplPhys*, 53 (2015) 102.

3 Kimijima T, Kanie K, Nakaya M & Muramatsu A, *Appl Catal B: Environ,* 144 **(**2014) 462.

4 Gaikwad S S, Borhade A V & Gaikwad V B, *Der Pharma Chemica*, 4 **(**2012) 184.

5 Kimijima T, Kanie K, Nakaya M & Muramatsu A, *Cryst Eng Commun,*16 **(**2014) 5591.

6 Kim J S, Cheon C I, Kang H J, Lee C H, Kim K Y, Nam S & Byun J D, *Jpn J Appl Phys,* 38 (1999) 5633.

7 Mi G, Murakami, Shindo D & Saito F, *Powder Technol,* 104 **(**1999) 75.

8 Gralik G, Thomsen A, Moraes C A, Raupp-Pereira F & Hotza D, *Process Appl Ceram,* 8 (2014) 53.

9 Yin S, Chen D, Tang W & Yuan Y, *J Mater Sci*, 42 (2007) 2886.

10 Gu Q, Chen B, Lian Y, Pan Y & Wang A, *Integrated Ferroelectrics,* 163 (2015) 8.

11 Lemanski K & Deren P J, *J Lumin*, 145 (2014) 661.

12 Lee B D, Yoon K H, Kim E S & Kim T H, *Jpn J Appl Phys*, 42 **(**2003) 6158.

13 Muthuraman M, Patil K C, Senbagaraman S & Umarji A M, *Mater Res Bull,* 31 (1996) 1375.

14 Cavalcante L S, Maeques V S, Sczancoski J C, Escote M T, Joya M R, Varela J A, Santos M R M C, Pizani P S & Longo E, *Chem Eng J*, 143 (2008) 299.

15 TurkyA O, Rashad M M, Zaki Z I, Ibrahim I A & Bechelany M, *RSC Advances,* 5 (2015) 18767.

16 Lee S J, Kim Y C & Hwang J H, *J Ceram Process Res*, 5 (2004) 223.

17 Kutty T R N, Vivekanandan R & Murugraj P, *Mater Chem Phys,* 19 **(**1988) 533.

18 Meroni D, Porati L, Demartin F & Poleman D, *ACS Omega*, 2 (2017) 4972.

19 Dudhe C M, Nagdeote S B & Palikundwar U A, *Mater Res Bull*, 81 **(**2016) 43.

20 Dudhe C M, Nagdeote S B & Palikundwar U A, *J Alloys Compd*, 658**(**2016) 55.

21 Lemanski K, Gagor A, Kurnatowska M, Pazik R & Deren P J, *J Solid State Chem,*184 (2011) 2713.

22 Zhou M F, Bak T, Nowotny J, Rekas M & Sorrell C C, *J Mater Sci*, 13(2002) 697.

23 Li X, Zhang Q, Ahmad Z, Huang J, Ren J, Weng W, Han G & Mao C, *J Mater Chem B*, (2015).DOI: 10.1039/c5tb01158b.

24 Oliveria L H, de Moura A P, Nogueira I C, Aguiar E C, Sequinel T, Rosa I L V, Longo E & Varela J A, *Mater Res Bull,* 81 (2016) 1.

25 Boruc Z, Fetlinski B, Malinowski M, Turczynski S & Pawlak D, *Opt Mater,* 34 **(**2012) 2002.

26 Vijaykumar M, Mahesvaran K, Patel D K, Arunkumar S & Marimuthu K, *Opt Mater,* 37 (2014) 695.

27 Malinowski M, Myziak P, Piramidowicz R, Pracka I, Lukasiewicz T, Surma B, Kaczmarek S, Kopczynski & Mierczyk Z, *Acta Physica Polonica A,* 90 (1996) 181.